

Data-Folding and Hyperspace Coding for Multi-Dimensional Time-Series Data Imaging

Chao Lian, Yuliang Zhao*, Zhikun Zhan, and Wen J. Li*, *Fellow, IEEE*

Abstract—Time-series classification and prediction are widely used in many applications. However, traditional machine learning algorithms, due to their limitations, have difficulty improving the performance of time-series classification and prediction. Inspired by the recent successes of the deep learning technology in computer vision, we develop a new time-series image encoding method for data reconstruction. Featuring data-folding and hyperspace coding this method breaks the barriers between time-series signals and images and establishes a close relationship between them, allowing effective application of the deep learning technology for time-series data. Besides a raw data coding method, we also present other four extended coding methods for other potential applications. For comparison purposes, we present the results of the five different types of image coding methods with our previous keystroke recognition datasets. The results show that our method can achieve an impressive accuracy of 96.27% when RGB coding images are used, and an accuracy of up to 97.33% when using radon coding way. We can expect that this method can also be used and perform well in other classification and prediction applications.

Index Terms—Human activity recognition (HAR), smart ring, machine learning, hierarchical decision.

I. Introduction

Sensor sensing technology is one of the three pillars of modern information industry and an important milestone in the evolution of science and technology. Real-world applications such as motion recognition [1][2], fault diagnosis [3][4][5], and medical care [6][7] can produce multi-dimensional time-series data that requires processing.

This work was supported by the National Natural Science Foundation of China (Grant No.61873307), the Hebei Natural Science Foundation (Grant No. This work was supported by the National Natural Science Foundation of China (Grant No.61873307), the Hebei Natural Science Foundation (Grant No. F2020501040, F2021203070, F2021501021), the Fundamental Research Funds for the Central Universities under Grant N2123004, the Administration of Central Funds Guiding the Local Science and Technology Development (Grant No. 206Z1702G) and in part by the Chinese Academy of Sciences (CAS)-Research Grants Council (RGC) Joint Laboratory Funding Scheme under Project JLFS/E-104/18. (Corresponding author: Y. Zhao and Wen J. Li.).

Z. Zhan are with School of Electrical Engineering, Yanshan university, Qinhuangdao 066004, China.

C. Lian and Y. Zhao is with the School of Information Science and Engineering, Northeastern University, Shenyang 110000, China, and Hebei Key Laboratory of Micro-Nano Precision Optical Sensing and Measurement Technology, Qinhuangdao, 066004, China (e-mail: zhaoyuliang@neuq.edu.cn).

Wen J. Li is with the CAS-CityU Joint Laboratory for Robotic Research, City University of Hong Kong, Hong Kong, SAR, Chin (e-mail: wenjli@cityu.edu.hk).

However, this problem has not been well solved due to the lack of a universal cross-domain fusion framework for such multi-modal sensor data.

Recently, due to its strong ability in feature extraction, the deep learning technology has achieved great successes in processing time-series data from different applications. To apply this technology in time-series classification with high accuracy, many researches have been conducted and a list of achievements have been made. For example, Karim, F [8] proposed a method that augmented fully convolutional networks with LSTM sub-modules for time-series classification, which achieved improved performance. A. Chowdhury [9] using 1D Triplet Convolutional Neural Network (1D-Triplet-CNN) to fused features from time series data for enhancing the performance of speaker recognition in challenging scenarios. C. Xiao [10] presented DeepSeg, a deep learning-based activity segmentation framework for activity recognition using WiFi time-series data. K. Wang [11] modified the traditional convolutional neural network (CNN) by the attention mechanism for activity recognition with time-series data. However, these researches still focus the recognition work on the raw time-series data, which limits the recognition performance of the deep learning technology.

To make better use of the excellent classification ability of CNN, some recent researches have explored a method where the time-series classification problem is transformed into an image classification problem by encoding time-series data into images [12][13][14]. By this method, the feature region of the sequence can be amplified to construct temporal correlation, thus improving the accuracy. For example, Z. Qin [15] converted acceleration data and angular velocity data into multi-channel GAF images, and then fused these images with a multi-branch residual network for human activity recognition. M. Ganesan [16] encoded time-series data into images using Gramian angular fields (GAF), and then analyzed the images by a convolutional neural network (CNN) for recognizing faulty and normal conditions of a satellite power system. Z. Ahmad [17] fused four types of activity images, i.e., Signal Images (SI), Gramian Angular Field (GAF) Images, Markov Transition Field (MTF) Images and Recurrence Plot (RP) Images, with a multimodal fusion framework for heart beat classification. Similarly, C. Yang [18] encoded multivariate time-series data into two-dimensional images with Gramian Angular Summation Field (GASF), Gramian Angular Difference Field (GADF), and Markov Transition Field (MTF), respectively, and then concatenated the images into one bigger image for classification through a CNN (ConvNet).

Although these image coding methods perform well in time-series data encoding, they are mostly suitable for one-dimensional time-series data. When it comes to multi-dimensional time-series data, these methods, such as GAF and GASF, can only encode a single channel of data at a time. To handle multi-dimensional time-series data with these

methods, several images must be generated, and then these images must be fused with some other images for classification. Therefore, it can be a challenging task to directly encode multi-dimensional time-series data in images into images for classification using a deep learning method.

In this paper, inspired by the features of colorful images, we propose a new Data-Folding and Hyperspace Coding method, the DFHC method for short, for multi-dimensional time-series data imaging. In a sensor environment, we find that all commonly used sensors, such as accelerometers and gyroscopes, produce 3-axis data, and there are exactly three channels of data in a colorful image. Therefore, we base our study on this idea and attempt to code these types of data from a new perspective. The contributions of this paper can be summarized as follows:

- 1) First, we proposed a new image coding method that can image multi-dimensional time-series data effectly.
- 2) Second, we extended our DFHC method into four different variations to explore its possible uses in other applications.
- 3) Third, we introduced a CNN network for classification of keystroke recognition data, through which we proved the effectiveness of our DFHC method.

II. METHOD

A. Data preparation

For the keystroke recognition task, we collected 12 channels of signals, including 3-axis acceleration data, 3-axis gyroscope data, 3-axis magnetometer data, and 3-axis euler angle data. As covered in our previous work, these signals have proved to be effective in detecting keystrokes[19][20]. For illustration purposes, we only adopted the keys typed by the left hand here in this paper to prove the effectiveness of our series-to-image framework. After the data was preprocessed, we finally conducted 25 experiments, in each of which two volunteers were asked to type 15 keys in random orders. Therefore, our work can be summarized as one that classifies these keystrokes using our proposed data imaging method.

B. Generation of keystroke fragments

After 12 channels of raw signals are collected, we segmented these signals into different fragments for each keystroke, so that these keystrokes could be recognized using a deep learning method. After segmentation, due to the need for images of the same size, it was necessary to adjust the different keystrokes into the same size. Based on our observation, there were around 150 points in the window of each key, so it was a good way to resize each keystroke with this window length. We used cubic spline interpolation to adjust signals into the same size. Then, we obtained 1500 pieces of time-series data of keystrokes for each subject. For keystroke recognition, the encoded time-series images were shuffled and 50% samples were adopted for training and the other 50% for testing.

C. Encoding data into images

Because different types of data have different dimensions, the data needed to be standardized to be between 0 and 1 before encoding. The raw data was set as $S(t)$, and then the formula can be written as:

$$X(t) = \frac{S(t) - \min(S)}{\max(S) - \min(S)} \quad (1)$$

Then we could get the new time-series data $X(t)$.

Each type of raw signal contains 3-axis data, and there are exactly three channels of data in a colorful image, i.e., R, G and B channels. Inspired by this idea, we could transform the raw data into a colorful image. Take acceleration data for example, the relationship between these two forms of data can be expressed as follows:

$$\text{Channel R: } I(1, :, 1) = \{ax_1, ax_2, \dots, ax_n\}$$

$$\text{Channel G: } I(1, :, 2) = \{ay_1, ay_2, \dots, ay_n\}$$

$$\text{Channel B: } I(1, :, 3) = \{az_1, az_2, \dots, az_n\}$$

With this coding method, we could obtain a single line of colorful images. And the same operation could also be conducted with gyroscope, magnetometer and euler angle signal. After encoding, there are only one lines in the image, which is also difficult for recognition. Thus, a better way is to fold this images with a Approximate square, which is more suitable for deep learning recognition. The method can be shown as follows:

Define each type of sensor data as one mode, and set the number of modes in the original data as M , and the data length of each dimension is set as L . Then the size of row and column of transformed images can be defined as:

$$W = \sqrt{M * L} \quad (2)$$

Where W represents the approximate number of lines after folding. In addition, since the m -mode data is folded simultaneously each time it is folded during the folding process, W needs to be an integer multiple of M .

Let the number of folds be N , then the relation between N and the number of rows W is:

$$N' \approx \frac{W}{M} \quad (3)$$

Considering that N can be a decimal, it is necessary to round N .

$$N = \text{floor}(N') \quad (4)$$

Where floor is a downward integral function. At this point, the number of folds can be obtained, and then the image P with rows and columns approximately $N * N$ can be obtained.

Finally, we can obtain a clear colorful images for recognition with deep learning method.

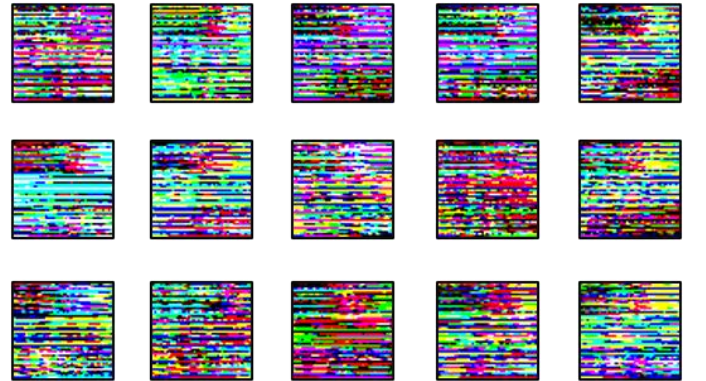


Fig. 1 RGB transformation images of 15 different keys.

D. Image evolution

Towards to different applying situation, the RGB image can be transformed into different type of forms, such as FFT image, DCT image and Radon image. For applying different situation, we should firstly transform the time series time before encoding rather than transform images directly.

1) FFT coding image

In some situations, time series observation cannot observe the internal state information, while Fourier transform can. So it is necessary to transform RGB images specially for this kind of scene with FFT coding method, which can help us observe the feature in the frequency domain.

Set $X(t)$ as raw time series data, then we conduct FFT transformation on it, the formula can be shown below:

$$F(u) = \sum_{t=0}^{T-1} X(t)W^{ut}, u = 0, 1, 2, \dots, T-1 \quad (5)$$

Where

$$W = e^{-j\frac{2\pi}{T}} \quad (6)$$

Finally, we get the absolute value of the Fourier transform as final result. Also, we move the zero-frequency component to the center of the spectrum for feature expression.

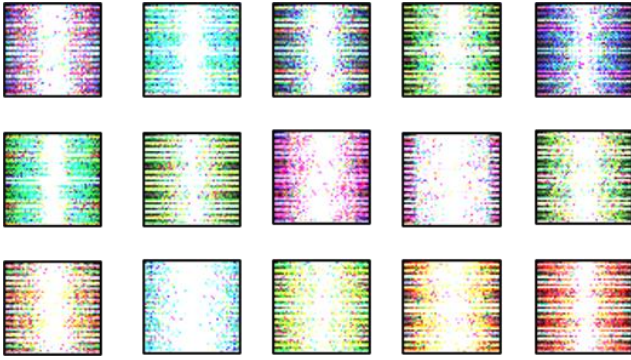


Fig. 2 FFT transformation images of 15 different keys.

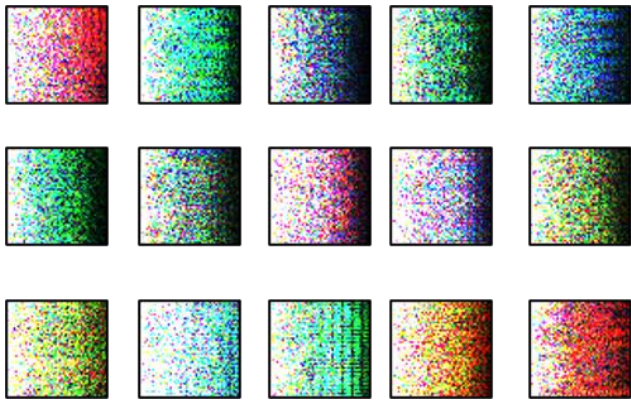


Fig. 3 DCT transformation images of 15 different keys.

2) DCT coding image

Through the study, it is found that in addition to the general orthogonal transformation property of DCT, the basis vector of its transformation matrix is very similar to the eigenvector of Toeplitz matrix, which reflects the related characteristics of image signals. So, DCT transformation is considered as a quasi-optimal transformation in the orthogonal transformation

matrix of speech and image signal transformation. The formula of DCT coding method can be shown below:

$$F(u) = C(u) \sqrt{\frac{2}{T}} \sum_{t=0}^{T-1} X(t) \cos \frac{(2x+1)u\pi}{2T}, u = 0, 1, \dots, T-1 \quad (7)$$

Where

$$C(u) = \begin{cases} 1/\sqrt{2} & u = 0 \\ 1 & u = 1, 2, \dots, T-1 \end{cases} \quad (8)$$

Finally, we get the absolute value of the DCT transform as final result.

3) Radon coding image

Radon transform is also an important image processing method, which means that the image function is integrated first along different lines in the plane, that is, projection transform is carried out. Then we can get the salient characteristics of the image in that direction. Set the pixel of image as $f(x, y)$, then the formula of Radon coding method can be shown below:

$$R(\rho, \theta) = \int_{-\infty}^{\infty} \int_{-\infty}^{\infty} f(x, y) \delta(x \cos \theta + y \sin \theta - \rho) dx dy \quad (9)$$

Where ρ represents the distance from the origin of the coordinates to the projection line L. θ is the angle between the normal line of L and the X-axis, which ranges from 0 to π .

Finally, we get the absolute value of the DCT transform as final result.

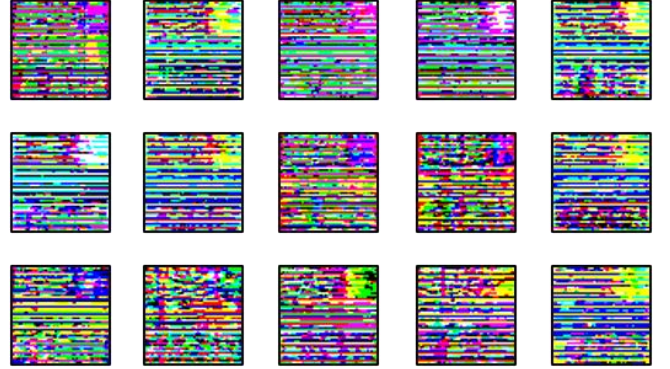


Fig. 4 Radon transformation images of 15 different keys.

4) Statistical coding image

For the original RGB image, we can see that the colors in the image are chaotic and it is hard to see the difference between different types by the naked eye. Therefore, an additional statistical coding method is proposed in this paper, that is, a new image can be obtained by sorting a channel (R, G or B) of each pixel by line. In this way, we can get three channel statistical encoded images with distinct differences.

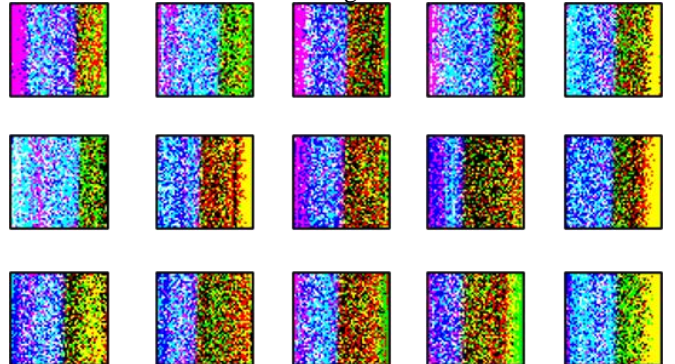


Fig. 5 Radon transformation images of 15 different keys.

According to the sorting results of different channels, we can get three different images after statistical coding. Then, for each channel, we set them as the different channel from a fusion colorful image.

III. ARCHITECTURE OF CONVOLUTIONAL NEURAL NETWORK

A. Structure of proposed deep learning architecture

For images recognition, we introduce convolutional neural network to recognize different keystrokes. After encoding the signals into images, it is resized as 50*48 pixel. Then this image consists of acceleration, grayscale, management and Euler angle are fed into the CNN model to classify the keystrokes.

The proposed architecture classifies the image by using the sequential operation of convolution and pooling layer; and transfers the activation values in one volume to another volume by means of a differentiable function. The convolutional kernels provide an output using the rectified linear unit (ReLU). The pooling layer reduces the amount of computation time and optimizes the parameters to acquire better accuracy. The number and sizes of the filter in the convolution and max-pooling layers are reported in Table 1. From Table 1, it is seen that the proposed model consists of four convolution layers and four max-pooling layers of size 2×2 .

The proposed deep learning model takes an image of size 50×48 pixel as an input and performs classification of 15 types of keys. In Table 1, the conv2D-1 to conv2D-4 are the convolutional layers that provide convolution operation while the max-pooling layers select the maximum value in one feature abstraction stage. The information is passed through a total of 4 convolutional layers, and the 4 max-pooling layers. Additionally, the two FC layers perform the desired computation when applying it after using the inner products of the neural network layer. Finally, the 15 neurons for 15 types of keys in the output layer with a softmax classifier predict the probability for each key class.

Table 1 Number and size of filters in the CNN networks

Layer name	Output shape	Parameter
Conv2D	$50 \times 48 \times 32$	2432
MaxPooling2D	$25 \times 24 \times 32$	0
Conv2D	$25 \times 24 \times 64$	18496
MaxPooling2D	$12 \times 12 \times 64$	0
Conv2D	$12 \times 12 \times 96$	55392
MaxPooling2D	$6 \times 6 \times 96$	0
Conv2D	$6 \times 6 \times 96$	83040
MaxPooling2D	$3 \times 3 \times 96$	0
Flatten	864	0
Dense	512	442880
Activation	512	0
Dense	15	7695
Classifier		softmax

B. Feature extraction via convolutional layer

The process of feature extraction using convolutional layer is discussed in this section. In the convolutional layers, the feature extraction procedure is staged by applying a 2D convolutional operation to the input image. The application of convolutional

operation to the input image changes the stride number for the horizontal and vertical direction, filter exploration movement range and the dimension size of the resulting image. Therefore, the filter size, number of filter, padding operation and stride values are the main factors need to be considered in the convolutional layer.

From Table 1, the conv2D-1 layer has 32 filters of size 50×48 and strides by 1 pixel unit in the horizontal and vertical directions. A max-pooling filter of size 25×24 with a stride of 2 pixel unit explores in the horizontal and vertical direction. The remaining conv2D-2 to conv2D-4 layer performs the operation with 64, 64 and 96 filters of size 25×24 , 12×12 , and 6×6 respectively with a stride by 2 pixel unit. The pool size of the first to fourth max pooling layer is selected as 2×2 . The term ReLU and softmax activation function is used in convolutional layer and output layer respectively. The function of ReLU activation function is to convert the nonlinear separable data to linear data which is fed to output layer. The proposed architecture successively applies the pooling operations and convolution filters to input data and creates a hierarchy of layers. The output of those layers are increasingly complex feature vectors than the input data which is necessary to simplify the data for obtaining high accuracy.

In the proposed methodology, every pixel is given as input of $n_1 \times 1$ for the input layer where n_1 defines the number of bands in eye image. The hidden convolution layer filters the $n_1 \times 1$ input vector through t kernels with the size of $k_1 \times 1$. The number of nodes in convolution layer can be defined as $t \times n_2 \times 1$, where $n_2 = n_1 - k_1$. The activation map of the convolutional layer can be represented as,

$$\tilde{y}^{i(r)} = \max \left(0, \tilde{b}^{j(r)} + \sum_j \tilde{k}^{ij(r)} * \tilde{x}^{i(r)} \right) \quad (10)$$

where, $\tilde{x}^{i(r)}$ = i th input activation map.

$\tilde{y}^{j(r)}$ = j th output activation map.

$\tilde{b}^{j(r)}$ = bias of the j th output map.

$\tilde{k}^{ij(r)}$ = convolution kernel between the i th input map and the j th output map.

C. Max pooling layer

Pooling layer decreases the size of the convolutional layers output. When passing through multiple pooling layers, a large image will be scaled down but keeps the features required for recognition. In max pooling layer the maximum value is stored. The max-pooling layer can be defined as,

$$\tilde{y}_{jk}^i = \max \left(\tilde{x}_{js+m, ks+n}^i \right) \quad (11)$$

Here, \tilde{y}_{jk}^i denotes a neuron in the i th output activation map, which is computed over a non-overlapping local region of size $(s \times s)$ in the i th input map.

D. Fully connected layer

In the fully connected layers, every neuron in layer l is fully connected to the outputs of all neurons in layer j . Each of the connections is necessitated for the calculation of the weighted sum. The output $y^{(l)j}$ of neuron j in a fully connected layer l is dependent on,

$$y_{jk}^i = \phi(x) \left(\sum_{i=1}^{n^{(l-1)}} y_i^{(l-1)} \cdot w^{(l)}(i, j) + b^{(l)}(j) \right) \quad (12)$$

Where $N^{(l-1)}$ defines the number of neurons in the previous layer ($l-1$), $w^{(l)}(i, j)$ is the weight for the connection from neuron i in layer to neuron j in layer l , $b^{(l)}(j)$ is the bias of neuron j in layer l and $\phi(x)$ is the activation function.

E. Softmax layer

Softmax classifier is applied to handle multi-class classification in the fully connected condition of the system. Assume that there are K classes and n labeled training sample. For each test input, the softmax classifier creates a K -dimensional vector whose elements sum to 1. Each element of output vector represents the estimated probability of each class label as follows,

$$P(y_i = m | x_i; W) = a_i = \frac{e^{w_m^T x_i}}{\sum_{j=1}^K e^{w_j^T x_i}} \quad (13)$$

where, $W = w_1, w_2, w_3, \dots, w_k$ are the parameters which is learned by the back-propagation algorithm. The cross entropy loss function is used as the cost function for the Softmax classifier and it can be calculated as,

$$J(W) = - \sum_{i=1}^N \sum_{j=1}^K y_{ij} \log \left(\frac{e^{w_j^T x_i}}{\sum_{m=1}^K e^{w_m^T x_i}} \right) \quad (14)$$

With N is the number of data points in the training set. Then, the gradient descent method is applied to solve the minimum of the $J(W)$ as,

$$\nabla_w J(W) = \sum_{i=1}^N x_i (a_i - y_i)^T \quad (15)$$

Finally, the parameters are updated as,

$$W^{new} = W^{old} - \eta \nabla_w J(W) \quad (16)$$

where, η is the learning rate.

IV. RECOGNITION RESULT

In this part, we investigated the performance with different image coding method on our keystroke datasets, in which 70% are used for training and 30% are used for testing. Result with RGB image

A. Result with RGB image

The neural network imitates the application of neurons that present in the human brain. The term weight is used as the strength of electrical signal, while the neurons are connected. The weight of the specific neuron is multiplied with the specific value given as input to the neuron. The summation of all weighted values associated to the next layer applies as a input for the activation function. In this kinds of networks, the interaction between the neurons affect the output neurons when a new data is inserted to the network. The inclusion of new data needs to optimize to comply with previous input. The back-propagation algorithm is applied to optimize the neuron weights in the proposed neural network architecture.

The popular adaptive moment estimation (Adam) optimizer is adopted to learn the proposed architecture that works based on the extension to the conventional stochastic gradient descent method(SGD). The term ‘‘Adam’’ derives from the adaptive moment estimation which is used to update the network

weights iteratively and, in turn, minimizes the loss function in each epoch. The conventional SGD computes on a random selection of data examples which is inefficient. On the other hand, the Adam optimizer computes the individual adaptive learning rates for the different parameters. The learning rate is set at 0.001.

At the beginning of the training procedure, the input data is labeled with the correct output class in advance. The labeled data sample passes through the neural network. The optimal paramters for the Adam optimizer are determined by conducting several experiments to obtain the lowest loss value and the highest accuracy.

The proposed model is trained for the 100 epochs with Adam optimization algorithm where the categorical cross-entropy cost function is used to obtain optimum result. After the training phase, the proposed model appears to be promising in performances with the generated RGB image dataset. The training and test classification accuracy and loss curve conferred in Fig. 6. Fig. 6 shows the loss and the accuracy curve on how the system learns at every epochs. It is seen that the accuracy reaches nearly to one after 100 epochs. It shows that the accuracy of the proposed approach is 96.27% and the loss is 0.0202. This loss value is optimum for the proposed model.

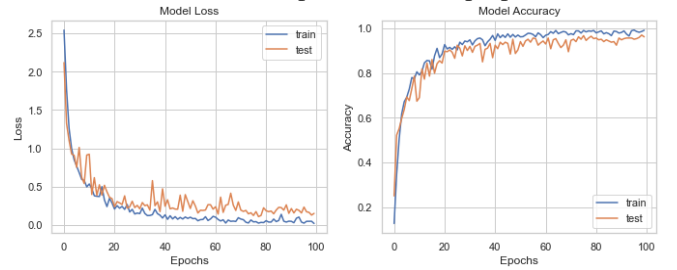


Fig. 6 The loss (left) and the accuracy (right) curve.

However, the average classification accuracy hides the details about the system performance. Thus the classification performance is further assessed with the confusion matrix as illustrated in Fig. 7; where a total of eleven different fault types are leveled along the x and y-axis of the 15×15 grids confusion matrix. The color depth of each grid signifies the percentage of correctly classified classes. The confusion matrix tells how the classifier performs for each class. From the confusion matrix, it is observed that the majority of the classes are classified correctly. Furthermore, we also present the ROC curve of this method, it can be seen that the area under the curve reaches to 0.98, which is impressive. As the overall accuracy, it is concluded that the proposed classifier is capable of classifying the keystrokes with quite high accuracy.

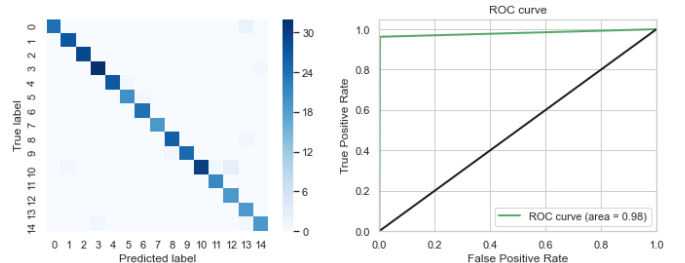


Fig. 7 Confusion matrix and ROC curve of RGB images.

B. Result with extended image

Different image coding method can show different performance toward to data that from special situation. To test

the performance in our keyboard situation, we additionally adopt extended image coding method for comparison.

1) FFT coding image

Fast Fourier transform can reflect the frequency domain characteristics of the signal. Based on this feature, we also recognized keystrokes with FFT coding image. The results are shown in Fig. 8. Fig. 8 shows recognition performance at every epochs. It is seen that the accuracy reaches nearly to one after 100 epochs. The accuracy of the this type of extended image is 86.13% and the loss is 0.2451. This loss value is optimum for the proposed model. Form confusion matrix, we can see that, this method can also relatively classify the keystrokes overall, while for some keys, the recognition accuracy are not as high as RGB images. However, the roc curve show a high performance which is 0.93.

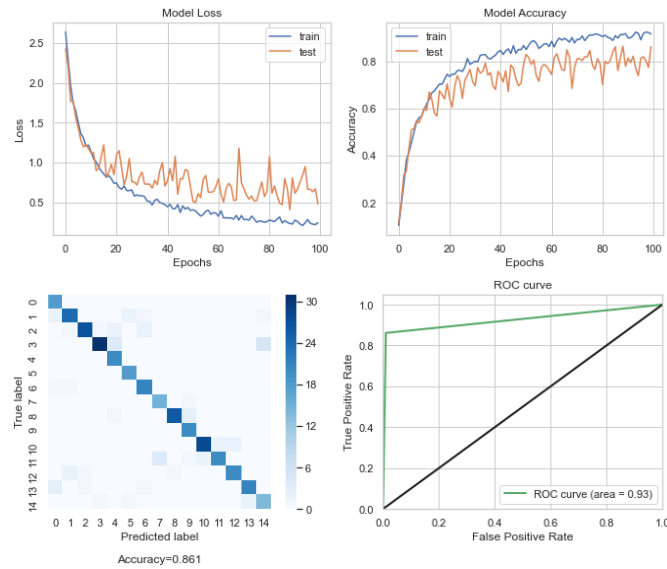


Fig. 8 Recognition performance with FFT coding image. (a) The loss and the accuracy curve(upper), (b) Confusion matrix and ROC curve(lower).

2) DCT coding image

DCT transform is an upgraded version of Fourier transform, which can also be used to reflect the frequency domain information of the signal. The results of this coding method are shown in Fig. 9. It is seen that the accuracy reaches nearly to one after 100 epochs. The accuracy of the this type of extended image is 65.07% and the loss is 0.6938. This loss value is optimum for the proposed model. Form confusion matrix, we can see that, this method cannot recognize the keystrokes well, because that for some keys this method lose the ability to recognize them. The roc curve also show a poor performance, which is only 0.81.

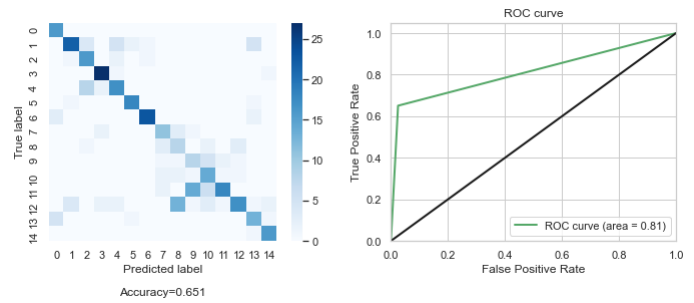


Fig. 9 Recognition performance with DCT coding image. (a) The loss and the accuracy curve(upper), (b) Confusion matrix and ROC curve(lower).

3) Randon coding image

Randon transform is a projection transformation based on different angles, which helps us get new features. As shown in Fig. 4, after transformation, new features are obtained at the upper right corner of the transformed image, namely feature blocks with strong distinguishing power. The results of this coding method are shown in Fig. 10. It is seen that the accuracy reaches nearly to one after 100 epochs. The accuracy of the this type of extended image is 97.33% and the loss is 0.0237. This loss value is optimum for the proposed model. Form confusion matrix, we can see that, this method can recognize the keystrokes well, which is even a little better than that of RGB images. What is more, the roc curve also show a poor performance, which is only 0.99, which is higher than all the other type of coding method.

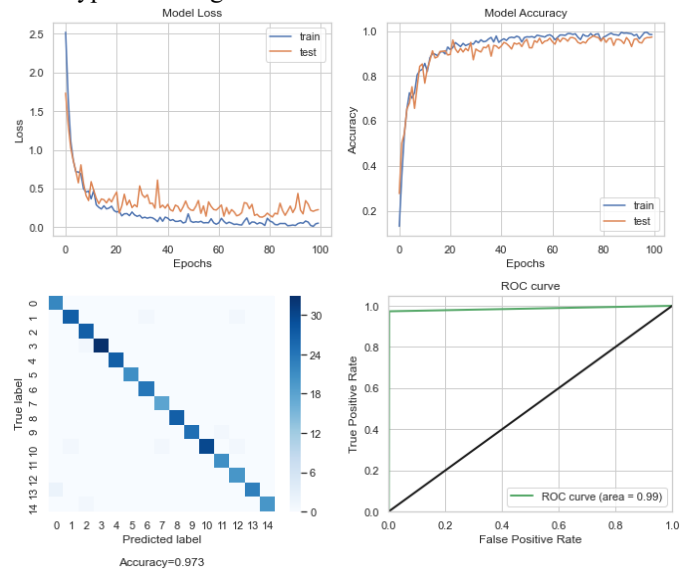
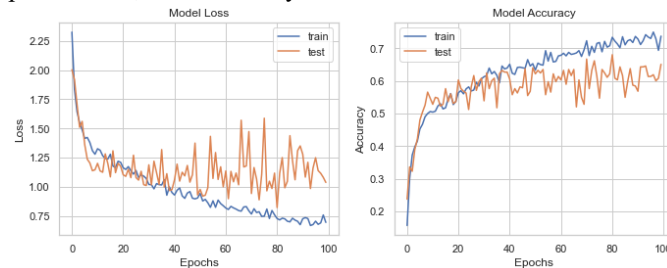


Fig. 10 Recognition performance with 3) Randon coding image. (a) The loss and the accuracy curve(upper), (b) Confusion matrix and ROC curve(lower).

4) Stastics coding image

The principle of statistical coding method is to encode the RGB image to improve the image identification ability while trying to obtain a new feature expression. The results of this coding method are shown in Fig. 11. It is seen that the accuracy reaches nearly to one after 100 epochs. The accuracy of the this type of extended image is 84.27% and the loss is 0.3079. Form confusion matrix, we can see that, this method can recognize some of the keystrokes well. However, for some keys the recognition result is poor. However, the roc area show a high value, which reaches to 0.92.



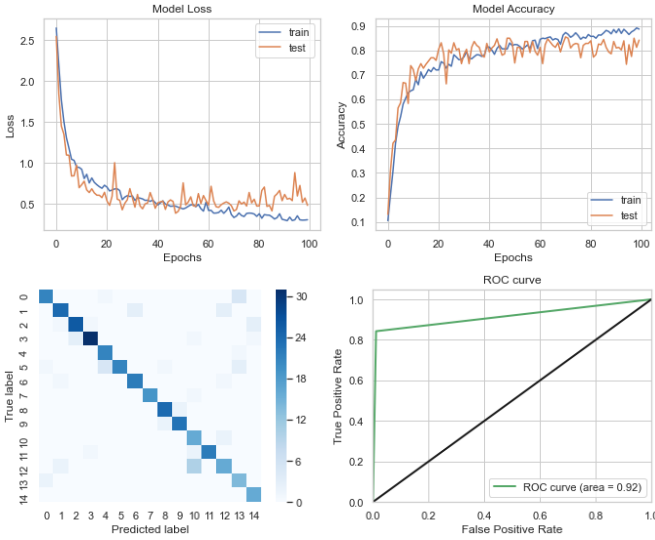


Fig. 11 Recognition performance with Statistics coding image. (a) The loss and the accuracy curve(upper), (b) Confusion matrix and ROC curve(lower).

C. Discussion

1) Evaluation metrics

To verify the efficiency of the proposed method, the following metrics are utilized, i.e., precision, sensitivity (recall), accuracy and F1 score.

$$\left\{ \begin{array}{l} \text{precision} = \frac{TP}{TP + FP}, \text{recall} = \frac{TP}{TP + FN} \\ \text{accuracy} = \frac{TP + TN}{TP + FN + FP + TN} \\ \text{F1-score} = 2 \times \frac{\text{precision} \cdot \text{recall}}{\text{precision} + \text{recall}} \end{array} \right. \quad (17)$$

where TP (true positive) is the number of positive samples predicted to be positive. FN (false negative) is the number of positive samples predicted to be negative. FP (false positive) is the number of negative samples predicted to be positive, and TN (true negative) is the number of negative samples predicted to be negative. Above four numbers also construct the confusion matrix, which is one of the evaluation indexes of various classification models. Additionally, the area under curve (AUC) of the receiver operating characteristic (ROC) is also employed to evaluate the overall performance of the proposed approach. In ROC, the true positive rate (TPR) is as a function of the false positive rate (FPR).

2) Evaluation result

We adopt the five image coding method and CNN model for comparison, and discuss with which one is more suitable for our situation. The result is shown in table 2.

Table 2 recognition results with different image coding method with CNN networks.

Coding type	Precision	Recall	F1-score	AUC	Accuracy
RGB	0.97	0.96	0.96	0.98	0.9627
FFT	0.87	0.86	0.86	0.93	0.8613
DCT	0.69	0.65	0.65	0.81	0.6507
Radon	0.97	0.97	0.97	0.99	0.9733
Statistic	0.86	0.84	0.84	0.92	0.8427

Table. 2 indicates the recognition results for different coding method. It can be seen that the overall performance of each case is well with high accuracy. The comparison shows that the result of Radon image outperforms the other three images by using total metrics as the evaluation indicator. Also, the RGB image also performs well in recognition keystrokes, which achieves the accuracy of 96.27% and AUC of 0.98. It is noteworthy that the FFT, DCT and statistic images have a relatively low performance, especially for DCT images (65.07%), which is caused by an enormous amount of misclassified samples. So, we can conclude that for our keystroke recognition datasets, RGB and Radon coding method are more suitable than other method.

However, it is not to say that FFT, DCT and Statistic method are always show poor performance. In our view, it is more creditable that different situations may be suitable for different image coding method. So, FFT, DCT and Statistic coding method may be more suitable for situations, such as fault diagnosis, vibration analysis, which is more needed for frequency domain analysis method.

V. CONCLUSION

In this study, a novel series to image architecture is put forward to detecting multiple types of series data, such as keystroke recognition situation. The raw time series are encoded as two-dimensional image vectors by using RGB, FFT, DCT, Radon and Statistic method. Moreover, in order to better distinguish different samples, a CNN model is designed and introduced. According to the analysis results from our keyboard datasets, RGB and Radon coding method perform better in our keyboard datasets, which reaches the accuracy of 96.27% and 97.33% respectively. And we can expect that, for different situation, the best coding method may be different. That is to say, our coding method proposed a good paradigm for multi-sensor data to image for high recognition performance.

REFERENCES

- [1] X. Hu, H. Zeng, A. Song, and D. Chen, "Robust Continuous Hand Motion Recognition Using Wearable Array Myoelectric Sensor," *IEEE Sens. J.*, vol. 21, no. 18, pp. 20596–20605, 2021.
- [2] C. Lian *et al.*, "ANN-Enhanced IoT Wristband for Recognition of Player Identity and Shot Types Based on Basketball Shooting Motion Analysis," *IEEE Sens. J.*, vol. 22, no. 2, pp. 1404–1413, 2022.
- [3] Z. Zhang and B. Xiao, "Sensor Fault Diagnosis and Fault Tolerant Control for Forklift Based on Sliding Mode Theory," *IEEE Access*, vol. 8, pp. 84858–84866, 2020.
- [4] A. Qin, Q. Hu, Y. Lv, and Q. Zhang, "Concurrent Fault Diagnosis Based on Bayesian Discriminating Analysis and Time Series Analysis with Dimensionless Parameters," *IEEE Sens. J.*, vol. 19, no. 6, pp. 2254–2265, 2019.
- [5] Y. Peng, W. Qiao, L. Qu, and J. Wang, "Sensor Fault Detection and Isolation for a Wireless Sensor Network-Based Remote Wind Turbine Condition Monitoring System," *IEEE Trans. Ind. Appl.*, vol. 54, no. 2, pp. 1072–1079, 2018.
- [6] Y. Bao, Z. Tang, H. Li, and Y. Zhang, "Computer vision and deep learning-based data anomaly detection method for structural health monitoring," *Struct. Heal. Monit.*, vol. 18, no. 2, pp. 401–421, 2019.
- [7] M. Li, "Human blood pressure measurement and medical care based on wireless sensors," *Microprocess. Microsyst.*, vol. 80, no. 2, p. 103649, 2021.

- [8] F. Karim, S. Majumdar, H. Darabi, and S. Chen, "LSTM Fully Convolutional Networks for Time Series Classification," *IEEE Access*, vol. 2017, no. 6, pp. 1662–1669, 2017.
- [9] A. Chowdhury and A. Ross, "Fusing MFCC and LPC Features Using 1D Triplet CNN for Speaker Recognition in Severely Degraded Audio Signals," *IEEE Trans. Inf. Forensics Secur.*, vol. 15, pp. 1616–1629, 2020.
- [10] C. Xiao, Y. Lei, Y. Ma, F. Zhou, and Z. Qin, "Deepseg: Deep-learning-based activity segmentation framework for activity recognition using wifi," *IEEE Internet Things J.*, vol. 8, no. 7, pp. 5669–5681, 2021.
- [11] K. Wang, J. He, and L. Zhang, "Attention-based convolutional neural network for weakly labeled human activities' recognition with wearable sensors," *IEEE Sens. J.*, vol. 19, no. 17, pp. 7598–7604, 2019.
- [12] S. Barra, S. M. Carta, A. Corriga, A. S. Podda, and D. R. Recupero, "Deep learning and time series-To-image encoding for financial forecasting," *IEEE/CAA J. Autom. Sin.*, vol. 7, no. 3, pp. 683–692, 2020.
- [13] W. Jiang, Y. Hong, B. Zhou, X. He, and C. Cheng, "A GAN-Based Anomaly Detection Approach for Imbalanced Industrial Time Series," *IEEE Access*, vol. 7, pp. 143608–143619, 2019.
- [14] J. Seon, Y. Sun, S. Kim, and J. Kim, "Time-lapse image method for classifying appliances in nonintrusive load monitoring," *Energies*, vol. 14, no. 22, p. 7630, 2021.
- [15] Z. Qin, Y. Zhang, S. Meng, Z. Qin, and K. K. R. Choo, "Imaging and fusing time series for wearable sensor-based human activity recognition," *Inf. Fusion*, vol. 53, pp. 80–87, 2020.
- [16] M. Ganesan and R. Lavanya, "A deep learning approach to fault detection in a satellite power system using Gramian angular field," *Int. J. Eng. Syst. Model. Simul.*, vol. 12, no. 2/3, p. 195, 2021.
- [17] Z. Ahmad and N. Khan, "Inertial Sensor Data to Image Encoding for Human Action Recognition," *IEEE Sens. J.*, vol. 21, no. 9, pp. 10978–10988, 2021.
- [18] C. L. Yang, Z. X. Chen, and C. Y. Yang, "Sensor classification using convolutional neural network by encoding multivariate time series as two-dimensional colored images," *Sensors (Switzerland)*, vol. 20, no. 1, p. 168, 2019.
- [19] Y. Zhao, C. Lian, X. Zhang, X. Sha, G. Shi, and W. J. Li, "Wireless IoT Motion-Recognition Rings and a Paper Keyboard," *IEEE Access*, vol. 7, pp. 44514–44524, 2019.
- [20] C. Lian *et al.*, "Towards a Virtual Keyboard Scheme based on Wearing One Motion Sensor Ring on Each Hand," *IEEE Sens. J.*, vol. 21, no. 3, pp. 3379–3387, 2020.